D. BOCHENEK[1], P. NIEMIEC[1*], D. BRZEZIŃSKA[1]

ELECTROPHYSICAL PROPERTIES OF THE MULTIFERROIC BFN-FERRITE COMPOSITES OBTAINED BY SPARK PLASMA SINTERING AND CLASSICAL TECHNOLOGY

In the paper the multiferroic (ferroelectric-ferromagnetic) composites based on ferroelectromagnetic/ferroelectric ($BaFe_{1/2}Nb_{1/2}O_3$ (BFN)) powder and ferrite powder (zinc-nickel ferrite) were obtained by two technological methods. In the composite samples the ratio of the ferroelectromagnetic/ferroelectric powder to the magnetic powder was equal to 90:10. The ceramic powders were synthesized by the classical technological method using powder calcination/solid state synthesis, while densification of the composite powders (sintering) was carried by two different methods: (i) Free Sintering method (FS), and (ii) Spark Plasma Sintering (SPS).

At the work, a comparison of measurement results for composite samples obtained by two sintering methods was made. The studies included the following analysis: DTA, XRD, SEM, DC electrical conductivity, electric permittivity and magnetic properties. The result of measurements presented in the work revealed that the ceramic composite obtained by two different technological sintering method (classical technology – Free Sintering method and Spark Plasma Sintering technique) can be promising lead-free materials for functional applications, for example in sensors for magnetic and electric field.

Keywords: Multiferroic composites; BFN ceramics; Spark Plasma Sintering (SPS)

1. Introduction

Ferroelectromagnetics are materials that have magnetic (ferromagnetic, ferrimagnetic, antiferromagnetic) and electrical (ferroelectric, ferrielectric, antiferroelectric) properties and belong to groups of multiferroics with various applications [1,2]. This group includes, for example: $Pb(Fe_{0.5}Nb_{0.5})O_3$, $Pb(Fe_{2/3}W_{1/3})O_3$, $Pb(Fe_{0.5}Ta_{0.5})O_3$ and multicomponent materials obtained on their basis [3-9]. Since the main component of these materials is lead, therefore, looking for lead-free materials with optimal parameters that can replace environmentally harmful lead materials is an important issue. The group of lead-free materials includes: $BaTiO_3$, $SrTiO_3$, $BiFeO_3$, $Bi_{0.5}Na_{0.5}TiO_3$, $K_{0.5}Na_{0.5}NbO_3$, $Na_{0.5}Bi_{0.5}TiO_3$, $BaFe_{0.5}Nb_{0.5}O_3$ and composites and multi-component compounds obtained on their basis [10-12].

Barium iron niobate $BaFe_{0.5}Nb_{0.5}O_3$ (BFN) is a relaxor ferroelectric material that has a diffuse phase transition (DPT) with a broad maximum in the temperature dependence of the dielectric constant. BFN material may be a good candidate for applications in electroceramic components such as high dielectric ceramic capacitors [13]. Nickel-zinc ferrite ($Ni_{0.64}Zn_{0.36}Fe_2O_4$ – in short (F)) belongs to the so-called soft ferrites, which exhibit high magnetic permeability, high dielectric constant, low dielectric loss, high resistivity, high Curie temperature, mechanical strength and chemical stability at relatively low frequencies. Soft ferrites are used, among others in electric machines for transforming electricity (transformers), generating electricity (alternators and generators, high frequency radar absorber materials (8-12 GHz) and catalysts, etc. [14,15].

In this work, two technological methods were used to obtain the BFN-F ceramic composites (in the weight ratio 9:1): (i) Free Sintering method (FS) and (ii) Spark Plasma Sintering (SPS). For the obtained composite samples, the following analyses were carried out: Differential Thermal Analysis (DTA), X-ray diffraction (XRD), Scanning Electron Microscopy (SEM), DC electrical conductivity, electric permittivity and magnetic properties.

[1] UNIVERSITY OF SILESIA IN KATOWICE, FACULTY OF SCIENCE AND TECHNOLOGY, INSTITUTE OF MATERIALS ENGINEERING, 75 PUŁKU PIECHOTY 1A, 41-500 CHORZÓW, POLAND

* Corresponding author: przemyslaw.niemiec@us.edu.pl
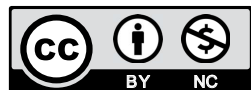
2. Experimental

2.1. Technological process

The main component of the BFN-F multiferroic composite was the ferroelectromagnetic $BaFe_{1/2}Nb_{1/2}O_3$ (BFN) material, whereas the second one was the magnetic $Ni_{0.64}Zn_{0.36}Fe_2O_4$ ferrite material (F). In the case of the BFN powder the starting reagents were barium carbonate $BaCO_3$ (99.99%, POCH), Nb_2O_5 (99.995%, Aldrich) and Fe_2O_3 (99.5%, Aldrich). The component powders were weighed according to the following reaction: $BaO +0.25Fe_2O_3+0.25Nb_2O_5 \rightarrow BaFe_{1/2}Nb_{1/2}O_3$, and next were milled in the planetary mill FRITSCH Pulverisette 6 for 24 h in ethanol. The mixture of the powders was synthesized at $T = 1250°C$ for $t = 4$ h by calcination method.

The second component of the multiferroic composite material was the $Ni_{0.64}Zn_{0.36}Fe_2O_4$ ferrite powder (F). The starting oxides NiO (99.99%, POCH), ZnO (99.995%, Aldrich) and Fe_2O_3 (99.5%, Aldrich) were milled in the planetary mill FRITSCH Pulverisette 6 for 24 h in ethanol using zirconia balls. The ferrite powder was obtained by the calcination method at 1000°C for 4 h.

In order to obtain the BFN-F multiferroic composite material, the synthesized powders of BFN and F materials were mixed (planetary mill, wet method in ethanol, for 8 h) in the weight ratio 9:1 and next calcined at 900°C for 2 h. The ceramic BFN-F multiferroic composites were obtained by two methods: (i) Free Sintering method (FS), and (ii) Spark Plasma Sintering (SPS). In the first method the sintering of the ceramic sample was carried out in the following conditions: 1050°C for 2 h (FSc sample), while in the second method the ceramic sample was carried out in the following conditions: temperature: 1000°C, time 3 min., pressure 50 MPa, atmosphere – argon, heating rate 50°C/min (SPSc sample).

The dimensions of the obtained samples were as follows: 10 mm in diameter and 1.5 mm thick (FSc samples), 12 mm in diameter and 10 mm thick (SPSc samples). The final steps of the technological process of the BFN-F multiferroic composites were grinding, polishing (after that all samples were 1.0 mm thick), annealing (removing mechanical stresses) and silver paste was deposition onto the both sample surfaces.

2.2. Investigations

The derivatographic analysis was performed on a Q-1500D derivatograph (F. Paulik, J. Paulik, L. Erdey system), in order to select the optimal conditions for the synthesis of the BFN-F composite powders (at temperature range of 20°C to 1050°C). The XRD test of the composite powder was carried out at room temperature (*RT*) on a diffractometer by PANanalytical Phillips X'Pert Pro. The X-ray diffraction patterns were done at range of 2q from 10° to 70° in step-scan mode: 0.05 degrees and 4 s/step and the copper radiations $CuK_{\alpha1}/_{\alpha2}$ were used. The SEM microstructure and EDS (Energy Dispersive Spectrometry) stud-

ies were made by a scanning electron microscopy JSM-7100F TTL LV (Jeol Lid., Tokyo, Japan). The surfaces of tested samples were coated with a layer of gold to provide electrical conductivity, in order to avoid charging effects. The dielectric tests were performed on the capacity bridge LCR Meter (Quad Tech 1929 Precision LCR Meter, Quad Tech, Inc. Maynard, USA), at temperature range of 20°C to 180°C (a heating cycle, a heating rate of 1.0 deg./min., frequency range of 1 kHz to 100 kHz). The measurements of DC electrical conductivity were carried out using a Keithley 6517B electrometer (Keithley Instruments, Cleveland, OH, USA), in the temperature range of 20°C to 350°C (a heating cycle). The magnetic measurements (the magnetic field up to 7 T) were carried in two parts, the first by a SQUID magnetometer (MPMS XL-7 Quantum Design) in the temperature range from –271°C to 27°C and second one, using a magnetic Faraday scale in the temperature range from 27°C to 600°C.

3. The results and discussion

Mixed BFN and ferrite powders after synthesis were subjected to derivatographic analysis. In the Fig. 1 on the DTA curve (Differential Thermal Analysis) the first peak at 70°C was due to the removal of water within micropores of the analysed powder. In the measuring range the TG (Thermogravimetry method) curve for the BFN-F composite powder shows gradual mass loss, leading to the total mass loss in an amount of 0.15%. The largest mass loss occurs in the temperature range from 564°C to 660°C, accompanied by small endothermic peaks in the DTA curve at 668°C.
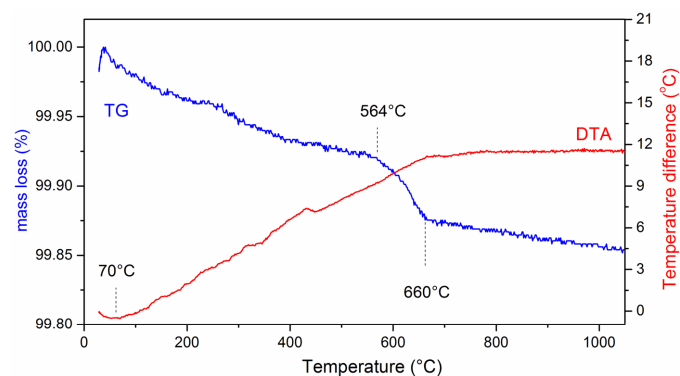

Fig. 1. DTA, TG curves of the BFN-F composite powder

The X-ray measurement at *RT* of the BFN-F composite material is depicted in Fig. 2. The X-ray analysis confirmed the occurrence of the strong diffraction peaks derived from the BFN ferroelectric matrix of composite and weak peaks from the ferrite component. In the case of the BFN the best fit was obtained to the model 00-057-0771 [16] with monoclinic perovskite structure ($a_0 = 4.074$ Å, $b_0 = 4.039$ Å, $c_0 = 2.876$ Å, $V = 47.32$ Å^3). In the case of the ferrite ($Ni_{0.64}Zn_{0.36}Fe_2O_4$) diffraction pattern shows a typical cubic spinel phase. The X-ray analysis confirmed the lack of a foreign phase.
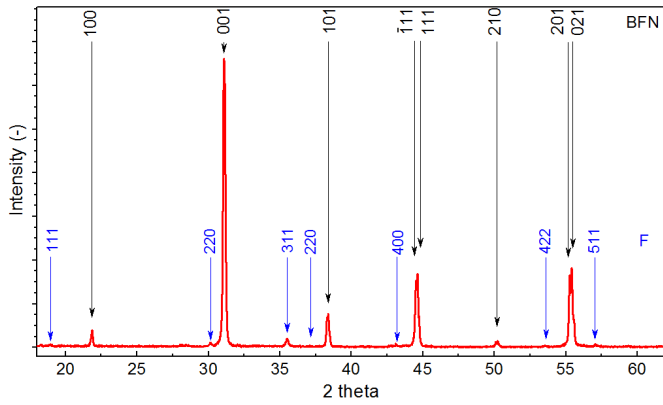
Fig. 2. XRD pattern of the BFN-F material

The microstructural images of fractures of composite samples are shown in Fig. 3. In the case of the FSc sample, large grains of the BFN (the ferroelectric component matrix) with sharp edges that surround the finer ferrite grains, also with clear edges, are observed. The ferrite grains in the BFN matrix are randomly distributed. The SPSc sample has a different microstructure. The BFN grains are fine with heterogeneous

shape and rough edges. The fine grains of the BFN ceramic component surround ferrite grains with fuzzy, irregular shapes. The above regularities are clearly visible in the SEM images of the composite samples obtained in the BSE (Back Scatterd Electron) technique – Fig. 4.

The BSE images of the microstructure of fractures, show the existence of the BFN matrix presented as bright elements (which is of higher atomic number) and ferrite grains presented as dark elements (with lower atomic number).

The EDS analysis of the BFN-F composite material (Fig. 5) was performed from ten randomly selected areas. Studies have shown that composite sample is free of impurities and that the chemical composition was relatively stable. The most stable behavior, in the BFN-ferrite composite, showed the chemical elements – barium (Ba), zinc (Zn) and nickel (Ni). Their content is close to 97-99% theoretical values. The concentrations of the chemical elements – niobium (Nb) and iron (Fe) are at about 95% of the theoretical values. The EDS studies have also shown higher oxygen content in the case of the SPSc sample.

Fig. 6 shows the $\ln \sigma_{DC}(1000/T)$ graph for the obtained BFN-F materials. It can be seen that the sintering method did not significantly affect the electrical conductivity. The use of
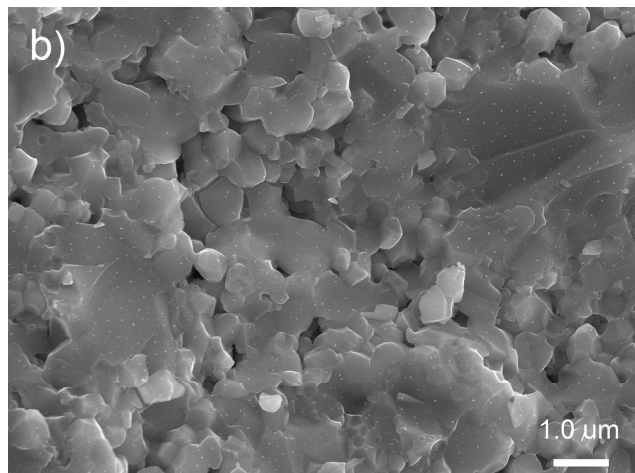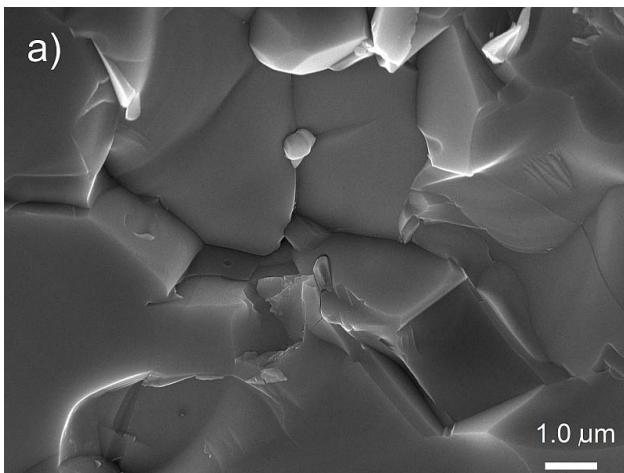

Fig. 3. SEM images of the microstructure of fracture of the BFN-F samples: FSc sample (a) and SPSc sample (b), at the standard SB mode
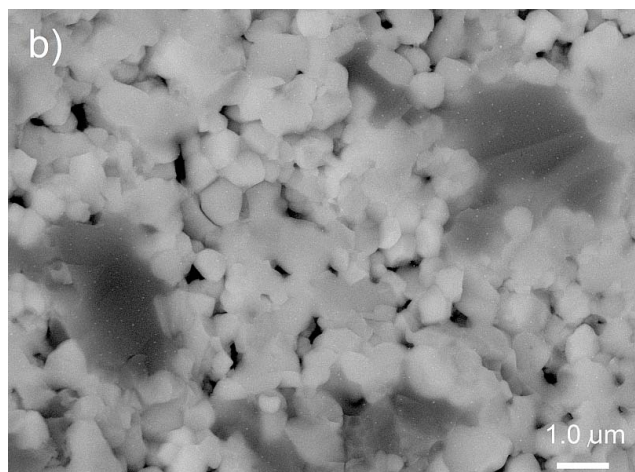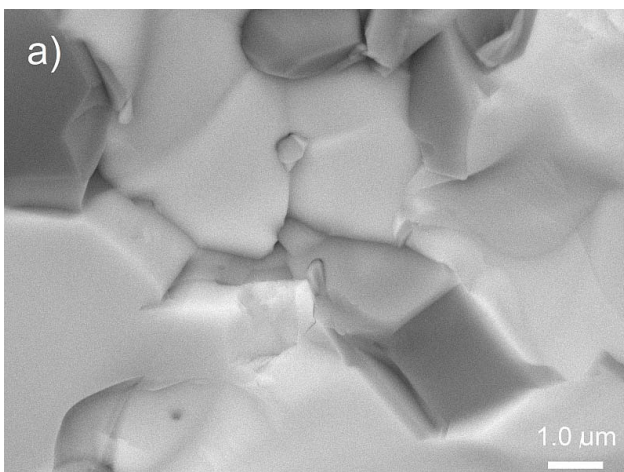

Fig. 4. BSE images of the microstructure of fracture of the BFN-F samples: FSc sample (a) and SPSc sample (b)
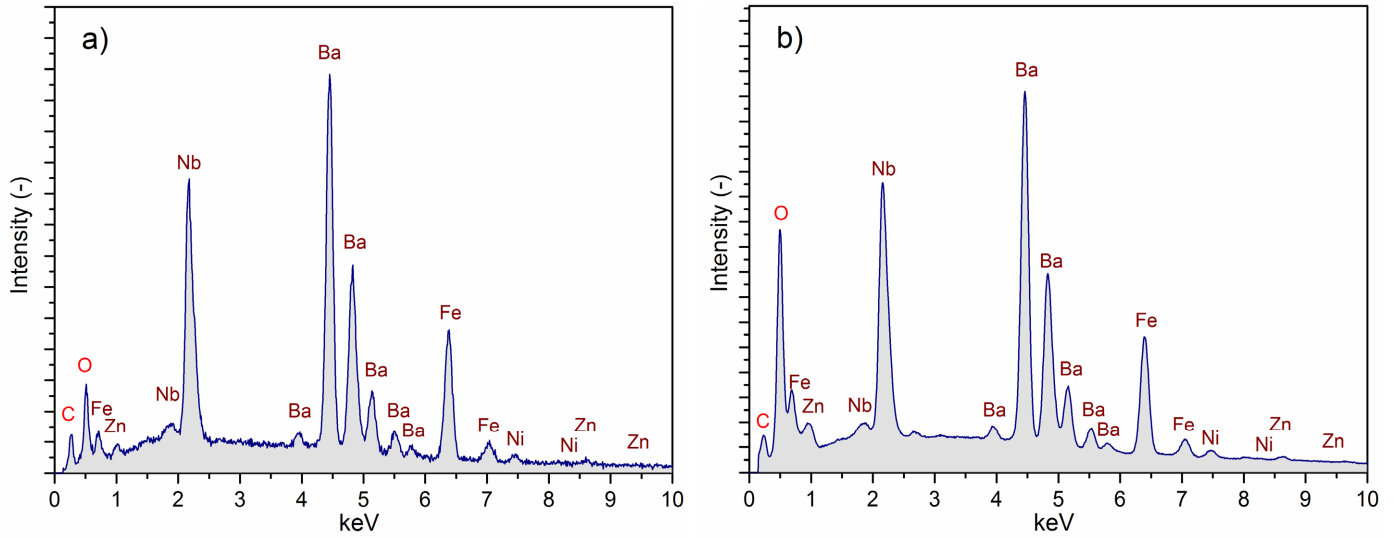
Fig. 5. The EDS analysis image of the element distribution for the BFN-F composite samples: FSc sample (a) and SPSc sample (b)
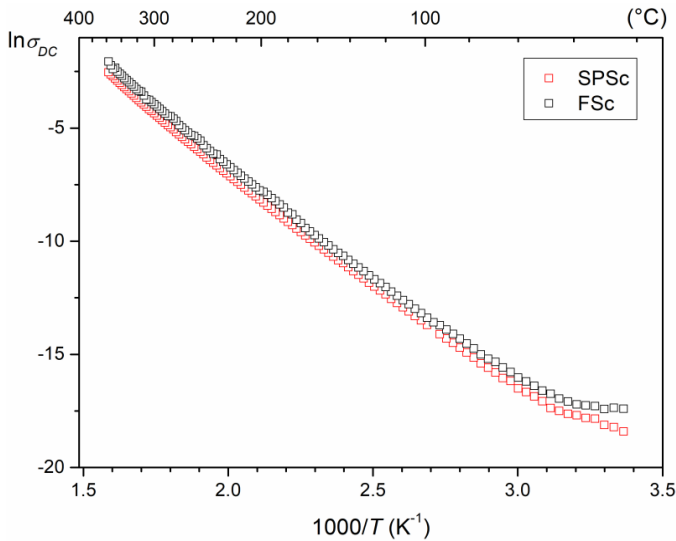

Fig. 6. The $\ln\sigma_{DC}(1000/T)$ dependences of the BFN-F composites

SPS method caused a very small decrease in conductivity in the BFN-F material. The temperature increase causes an increase in electrical conductivity for both of measured samples.

Temperature electric permittivity tests (Fig. 7) for the analysed composite samples showed a different character of the $\varepsilon(T)$. A sample of the FSc composite shows high values of electrical permittivity both at room temperature and at phase transition temperature (8305 at RT and 77568 at T_m, for 1 kHz). The phase transition is highly diffuse, with a maximum shift towards higher temperatures, as the measurement frequency increases. This is the so-called frequency dispersion characteristic of relaxor materials. The temperature T_m shift for the composite FSc sample in the 1 kHz to 100 kHz frequency range is 111°C (from 242°C to 353°C). With the increase in the frequency of the measuring field, the values of the maximum electric permittivity in T_m also decrease significantly, they are 77568 and 17760, respectively.
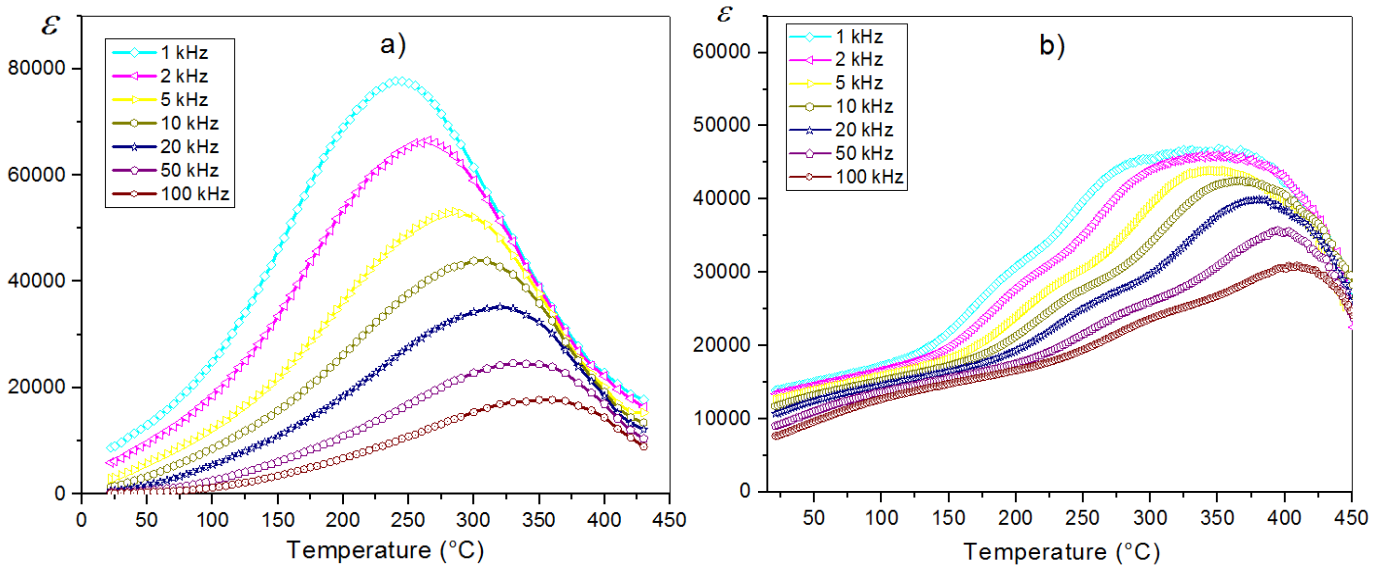

Fig. 7. The $\varepsilon(T)$ temperature relationships for the multicomponent BFN-F composites: FSc sample (a) and SPSc sample (b)

In the case of the composite sample obtained by the SPSc method, the temperature curves $\varepsilon(T)$ differ significantly from the sample obtained by the FSc method. At room temperature, the electric permittivity values of the SPSc sample are higher (14015, at 1 kHz), but at the phase transition temperature they are clearly lower (46680, at 1 kHz). Also the graphs $\varepsilon(T)$ for the SPSc samples show a strongly diffused phase transition. As the frequency of the measuring field increases, frequency dispersion is also observed (T_m shift towards higher temperatures), but it is not accompanied by a significant reduction in the value of electric permittivity (as was in the case of the FSc samples). The temperature T_m shift for the composite sample SPSc in the frequency range 1 kHz to 100 kHz is from 333°C to 410°C, respectively.

Fig. 8 presents the temperature dependence of dielectric loss for obtained composites. Studies have shown that the use of the SPS method in the technology of obtaining ceramic composites based on the BFN significantly reduces the dielectric loss of composite samples. For 1 kHz at room temperature the values of dielectric loss are 0.83 for the FSc sample, while for the SPSc sample they are an order of magnitude lower and 0.085. Low values of dielectric loss persist up to 200°C, after which the values of dielectric loss increase rapidly, which is associated with an increase in the electrical conductivity of composite samples.

Fig. 9 shows the temperature relationship of magnetization $M(T)$ of the BFN-F composite. The graph $M(T)$ presented characteristic areas with different properties. The first area about 400°C is associated with ferro/ferrimagnetic Curie temperature. The second one is associated with para/superparamagnetic properties, occurring at a temperature under –200°C. Above the temperature 480°C, the BFN-F composite is a paramagnetic material. The magnetic hysteresis loop of the BFN-F composite (at RT) is characteristic for soft ferromagnetic materials (Fig. 9 inside). In the range of weak magnetic fields an increase of the magnetization is caused by a growth of domains of a privileged direction of magnetization, at the expense of neighboring domains. This is the result of the so-called mechanism of domain's boundary shifting, which is a reversible process up to the point
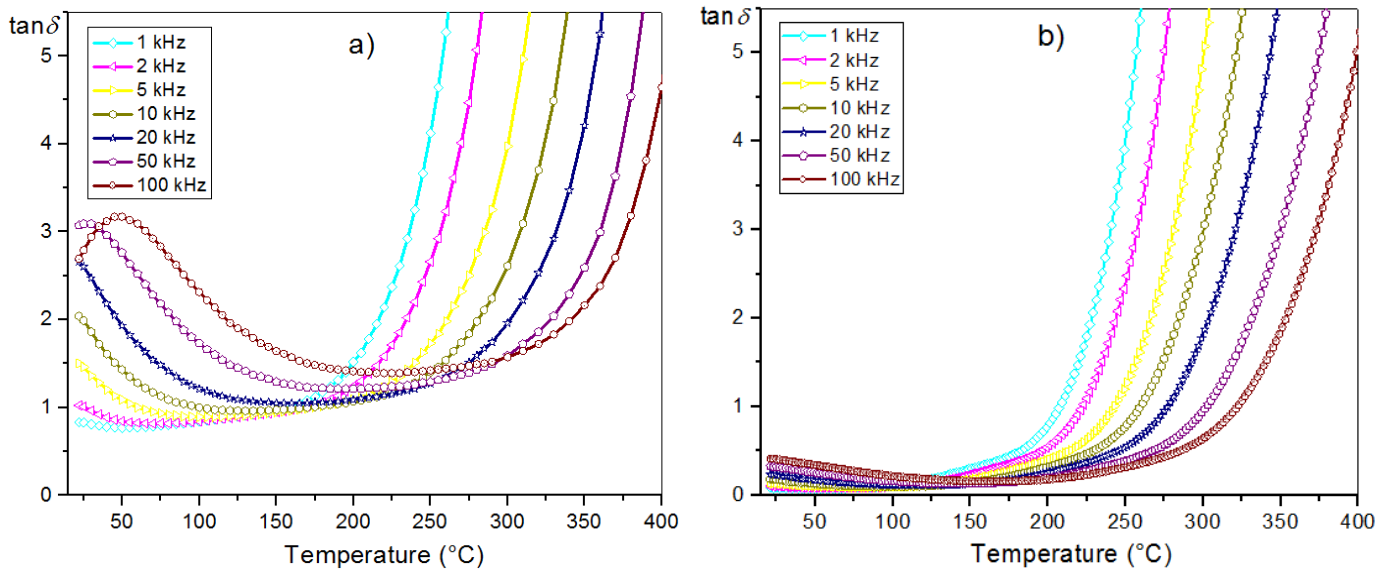

Fig. 8 Temperature dependences of the tand for the multicomponent BFN-F composites: FSc sample (a) and SPSc sample (b)
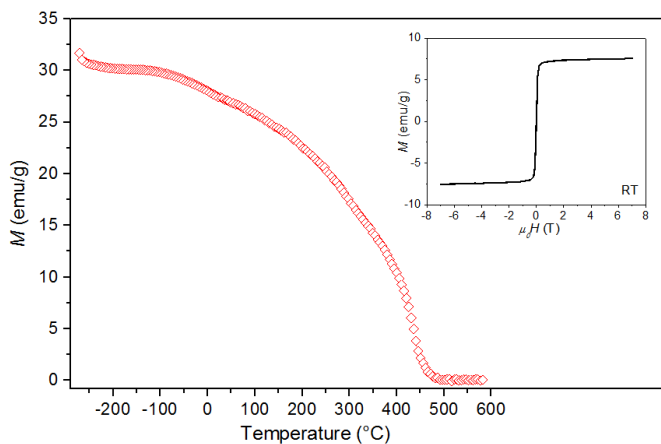

Fig. 9. Dependence of the $M(T)$ for the BFN-F composite (in the external 0.1 T magnetic field)

where the magnetic energy of the wall is comparable with the energy of magnetic interaction. In the range of stronger fields, the phenomena related to momentum rotations of particular areas of spontaneous magnetization show predominance (the sample's magnetization changes are irreversible), and saturation of the hysteresis loop is achieved in a proper magnetic field [17].

4. Conclusion

In this study the BFN-F multiferroic composites were prepared via the Free Sintering method (FS) and by Spark Plasma Sintering (SPS). The X-ray examinations confirmed the presence of strong peaks derived from the BFN (monoclinic perovskite structure) and weak peaks derived from ferrite (cubic spinel

phase). Microstructural studies have shown that the use of the SPS sintering allowed to obtain a fine-grained material (but with a heterogeneous shape of grains). With the conventional sintering method, large grain material was obtained. Sintering with the SPS method resulted in greater frequency dispersion and increased the degree of phase transition diffusion, compared with the Free Sintering method. Studies have shown that the use of the SPS method in the technology of obtaining ceramic composites based on the BFN significantly reduces the dielectric loss of composite samples. The Spark Plasma Sintering (SPS) is a method of fast sintering, however, choosing the right conditions is crucial in terms of improvement of electrophysical properties of the multiferroic composites.

REFERENCES

[1] M. Fiebig, T. Lottermoser, D. Meier, M. Trassin, Nat. Rev. Mater. **1**, 16046, 1-14 (2016).

[2] N.A. Spaldin. MRS Bull. **42**, 385-390 (2017).

[3] S. Sahoo, R.N.P. Choudhary, N. Kumar, B.K. Mathur, Solid State Sci. **14**, 6, 668-672 (2012).

[4] D. Bochenek, P. Guzdek, J. Magn. Magn. Mater. **323**, 3-4, 369-374 (2011).

[5] C.F. Yao, Z.Q. Liu, J.K. Shang, J. Alloy. Compd. **502**, 2 429-433 (2010).

[6] S. Matteppanavar, S. Rayaprol, B. Angadi, B. Sahoo, J. Alloy. Compd. **677**, 27-37 (2016).

[7] G. Alvarez, H. Montiel, J.A. Pena, M.A. Castellanos, R. Zamorano, J. Alloy. Compd. **508**, 2, 471-474 (2010).

[8] R. Font, O. Raymond-Herrera, L. Mestres, J. Portelles, J. Fuentes, J.M. Siqueiros, J. Mater. Sci. **51**, 6319-6330 (2016).

[9] W. Kleemann, P. Borisov, V.V. Shvartsman, S. Bedanta, EPJ Web Conf. 29, 00046, 1-8 (2012).

[10] S. Eitssayeam, U. Intatha, K. Pengpat, T. Tunkasiri, Curr. Appl. Phys. **6**, 3, 316-318 (2006).

[11] A. Mishra, D.K. Khatua, A. De. B. Majumdar, T. Frömling, R. Ranjan, Acta Mater. **164**, 761-775 (2019).

[12] Z. Wang, J.G. Wu, M. Xiao, D.Q. Xiao, T. Huang, B. Wu, F.X. Li, J.G. Zhu, Ceram. Int. **40**, 7, 9165-9169 (2014).

[13] P. Kantha, N. Pisitpipathsin, K. Pengpat, S. Eitssayeam, G. Rujijanagul, R. Gua, A.S. Bhalla, Mater. Res. Bull. **47**, 10, 2867-2870 (2012).

[14] O. Mirzaee, M.A. Golozar, A. Shafyei, Mater. Charact. **59**, 5, 638-641 (2008).

[15] A. Ghasemi, M.R. Loghman-Estarki, S. Torkian, M. Tavoosi, Compos. Part B-Eng. **175**, 107179, 1-15 (2019).

[16] S. Saha, T.P. Sinha, J. Phys., Condens. Matter. **14**, 249-258 (2002).

[17] D. Bochenek, P. Niemiec, A. Chrobak, G. Ziółkowski, A. Błachowski, Mater. Charact. **87**, 36-44 (2014).